



HAL
open science

Kerr-lens mode-locked Yb:SrLaAlO₄ laser

Zhang-Lang Lin, Huang-Jun Zeng, Ge Zhang, Wen-Ze Xue, Zhongben Pan, Haifeng Lin, Pavel Loiko, Hsing-Chih Liang, Valentin Petrov, Xavier Mateos, et al.

► **To cite this version:**

Zhang-Lang Lin, Huang-Jun Zeng, Ge Zhang, Wen-Ze Xue, Zhongben Pan, et al.. Kerr-lens mode-locked Yb:SrLaAlO₄ laser. *Optics Express*, 2021, 29 (26), pp.42837. 10.1364/OE.445574. hal-03858625

HAL Id: hal-03858625

<https://hal.science/hal-03858625v1>

Submitted on 17 Nov 2022

HAL is a multi-disciplinary open access archive for the deposit and dissemination of scientific research documents, whether they are published or not. The documents may come from teaching and research institutions in France or abroad, or from public or private research centers.

L'archive ouverte pluridisciplinaire **HAL**, est destinée au dépôt et à la diffusion de documents scientifiques de niveau recherche, publiés ou non, émanant des établissements d'enseignement et de recherche français ou étrangers, des laboratoires publics ou privés.



Kerr-lens mode-locked Yb:SrLaAlO₄ laser

ZHANG-LANG LIN,¹ HUANG-JUN ZENG,¹ GE ZHANG,¹
WEN-ZE XUE,¹ ZHONGBEN PAN,²  HAIFENG LIN,³ PAVEL LOIKO,⁴
HSING-CHIH LIANG,⁵ VALENTIN PETROV,⁶  XAVIER MATEOS,^{7,8} 
LI WANG,⁶  AND WEIDONG CHEN^{1,6,*} 

¹Fujian Institute of Research on the Structure of Matter, Chinese Academy of Sciences, 350002 Fuzhou, China

²Institute of Chemical Materials, China Academy of Engineering Physics, 621900 Mianyang, China

³College of Physics and Optoelectronic Engineering, Shenzhen University, 518118 Shenzhen, China

⁴Centre de Recherche sur les Ions, les Matériaux et la Photonique (CIMAP), UMR 6252

CEA-CNRS-ENSICAEN, Université de Caen, 6 Boulevard Maréchal Juin, 14050 Caen Cedex 4, France

⁵Department of Optoelectronics and Materials Technology, National Taiwan Ocean University, 202301 Keelung, Taiwan

⁶Max Born Institute for Nonlinear Optics and Short Pulse Spectroscopy, Max-Born-Str. 2a, 12489 Berlin, Germany

⁷Universitat Rovira i Virgili, Física i Cristal·lografia de Materials i Nanomaterials (FiCMA-FiCNA)-Marcel·lí Domingo 1, 43007 Tarragona, Spain

⁸Serra Hünter Fellow, Spain

*chenweidong@fjirsm.ac.cn

Abstract: We report on the first Kerr-lens mode-locked laser based on the Yb³⁺-doped disordered strontium lanthanum aluminate crystal, Yb:SrLaAlO₄ (Yb:SALLO), pumped by a high-brightness Yb fiber laser at 976 nm. Nearly Fourier-limited pulses as short as 44 fs were achieved at 1051 nm with an average output power of 277 mW and a pulse repetition rate of ~66 MHz via soft-aperture Kerr-lens mode-locking. A higher average output power of 459 mW, corresponding to an optical efficiency of 33.8%, was obtained at the expense of a slightly longer duration (52 fs).

© 2021 Optica Publishing Group under the terms of the [Optica Open Access Publishing Agreement](#)

1. Introduction

Disordered crystals represent an important class of materials for the design of tunable and ultrafast solid-state lasers. The dopant ions in such crystals experience significant inhomogeneous spectral broadening leading to smooth and very broad gain profiles. As structure disorder normally leads to deterioration of thermal properties, it is important to identify disordered gain media with high thermal conductivity. Among the disordered laser host crystals, the compounds with the chemical formula ABCO₄ (A²⁺ = Ca or Sr, B³⁺ = Y, Gd, La, etc., and C³⁺ = Al or Ga) crystallizing in the tetragonal system class with a K₂NiF₄ type structure (SG: *I4/mmm*) have recently come to the attention of researchers [1]. The structure disorder of these crystals originates from a random distribution of A²⁺ and B³⁺ cations over the same lattice sites; the inhomogeneous spectral broadening for the dopant ions is determined by their second coordination sphere [2]. Well-known examples of tetragonal ABCO₄ crystals are the rare-earth calcium aluminates CaREAlO₄, where RE³⁺ is an optically passive Y or Gd ion, abbreviated as CALYO or CALGO, respectively [3,4]. When doped with an active rare-earth ion, e.g., ytterbium (Yb³⁺), they exhibit a “glassy-like” spectroscopic performance but relatively high thermal conductivity and attractive thermo-optical properties (“athermal” behavior) [5]. This makes Yb-doped CALGO or CALYO crystals very suitable for power-scalable [6,7], broadly tunable and ultrafast lasers operation at ~1 μm [8–14]. In the mode-locked (ML) regime of operation, sub-20 fs pulses were generated from such crystals [15,16].

The search for other compounds in the $ABCO_4$ crystal family with improved thermo-mechanical properties is still ongoing. Very recently, an Yb^{3+} -doped strontium lanthanum aluminate crystal, $Yb:SrLaAlO_4$ (abbreviated: Yb:SALLO), was grown by the Czochralski method [17]. This crystal belongs to the same S. G. of the tetragonal system [lattice constants: $a = 3.7562(1)$ Å, $c = 12.6351(2)$ Å]. It is optically uniaxial and possesses high refractive index: $n_o = 1.916$, $n_e = 1.934$ at 670 nm [18,19]. Yb:SALLO exhibits high thermal conductivity ($\kappa_a = 6.1$, $\kappa_c = 4.3$ W/mK) for a disordered crystal together with broadband emission properties.

According to the quasi-three-level nature of the Yb laser, gain cross-section, σ_{gain} , spectra of Yb:SALLO were calculated for π -polarized light [17], as shown in Fig. 1. The extremely broad, flat and smooth spectral gain profiles indicate the high potential of Yb:SALLO for generation of sub-100 fs pulses from mode-locked lasers.

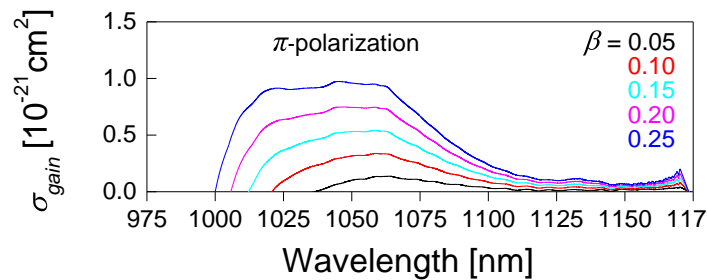


Fig. 1. Gain cross-section, σ_{gain} , spectra of Yb^{3+} in the SALLO crystal for π -polarization, β is the inversion ratio.

The excellent spectroscopic and thermo-mechanical properties of the Yb:SALLO crystal are attractive for passively ML operation in the 1 μ m spectral region. In this work, pumping with a high-brightness fiber laser at 976 nm, Yb:SALLO laser delivered pulses as short as 44 fs at 1051 nm via soft-aperture Kerr-lens mode-locking. To the best of our knowledge, this represents the first demonstration of ML operation of the Yb:SALLO laser.

2. Experimental configuration

Kerr-lens mode-locked (KLM) operation of the Yb:SALLO laser was investigated in a X-folded astigmatically compensated linear resonator, as shown in Fig. 2.

As a laser element, we used an a -cut Yb:SALLO crystal. This crystal orientation was selected to provide access to the desirable π -polarization which corresponds to stronger absorption at 976 nm and broader gain profiles (as compared to the σ -polarization). The actual doping level in the crystal was 1.18 at.% (the Yb^{3+} ion concentration $N_{Yb} = 1.36 \times 10^{20}$ cm $^{-3}$). The sample had an aperture of 3 mm \times 3 mm and thickness of 3.1 mm. It was mounted in a water-cooled Cu holder (coolant temperature: 20°C) and placed at Brewster's angle between two dichroic folding mirrors, M_1 and M_2 (radius of curvature, RoC = -100 mm). The crystal was polished from both sides and remained uncoated, and its orientation determined the π -polarized laser output.

The pump source was a 976 nm narrow-linewidth continuous-wave (CW) Yb fiber laser emitting a nearly diffraction-limited beam profile (beam propagation factor, M^2 of ~ 1.03) and linear polarization corresponding to $E \parallel c$ (π) in the crystal. A spherical lens (focal length, $f = 75$ mm) focused the pump beam into the laser crystal yielding a beam waist radius of 16 μ m \times 29 μ m in the sagittal and tangential planes, respectively. The cavity was completed by an additional folding mirror M_3 (RoC = -100 mm) and a flat rear mirror M_4 . The intracavity group delay dispersion (GDD) was managed by implementing a set of flat dispersive mirrors (DMs) with different negative GDD per bounce (DM $_1$ and DM $_2$: -250 fs 2 , DM $_3$ and DM $_4$: -100 fs 2). The

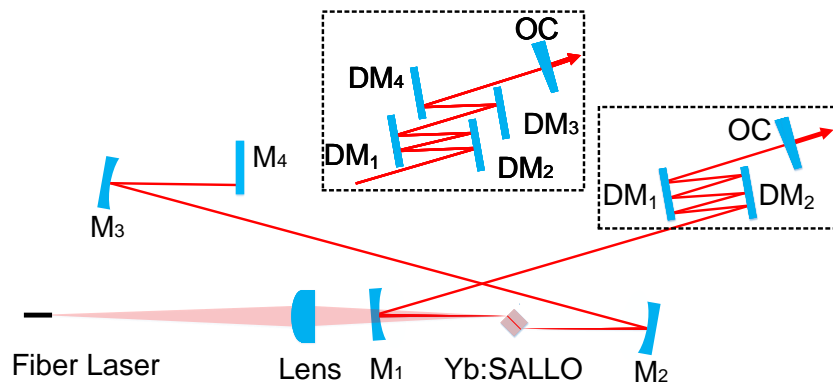


Fig. 2. Experimental setup of the KLM Yb:SALLO laser. Lens: spherical focusing lens ($f = 75$ mm); $M_1 - M_3$: dichroic concave mirrors ($\text{RoC} = -100$ mm), M_4 : flat rear mirror; $DM_1 - DM_4$: dispersive mirrors; OC: output coupler.

total negative GDD introduced by the DMs was varied by the number of bounces to balance the material dispersion, and the positive frequency chirp introduced by self-phase modulation (SPM) in ML operation. The group velocity dispersion (GVD) of the Yb:SALLO crystal was estimated from the dispersion curves [18] to be $\text{GVD} = 220 \pm 50 \text{ fs}^2/\text{mm}$ at $1.05 \mu\text{m}$ for π -polarization.

3. Experimental results

Initially, the Yb:SALLO laser was aligned for maximum output power in the CW regime when applying only four additional flat DMs ($DM_1 - DM_4$) which provided a total round-trip negative GDD of -2400 fs^2 . The maximum CW output power amounted to 1.03 W for a 4% OC at an absorbed pump power of 1.4 W. The measured single-pass pump absorption was around 29.8% due to the low Yb^{3+} doping level. Such low value originates from the non-optimum pump wavelength, away from the absorption maximum (980.2 nm), which would be one of the reasons for limiting the further scaling of the average power of the KLM Yb:SrLaAlO₄ laser. To discriminate the CW in favor of the ML regime of operation, the resonator was aligned towards the edge of the stability region through translating the folding mirror M_2 by several hundreds of micrometers away from the laser crystal. As a result, the CW output power dropped to 150 mW. The corresponding far-field laser beam profile captured using a CCD camera placed at 1.1 m from the OC was extended along the horizontal direction, see Fig. 3(a).

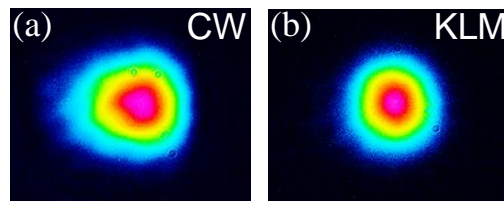


Fig. 3. Measured far-field beam profiles of the Yb:SALLO laser: (a) CW and (b) KLM regimes.

The transition from the CW to KLM regime was realized by applying a slight translation / knock of the flat rear mirror M_4 . The average output power experienced an abrupt increase up to 271 mW. A considerable change in the far-field beam profile was observed especially along the horizontal direction leading to a nearly symmetrical fundamental mode, see Fig. 3(b). The

recorded beam diameters changed from 2.6 (x) mm \times 2.2 (y) mm (CW regime) to 2.0 (x) mm \times 2.1 (y) mm (KLM regime), where x and y stand for the horizontal and vertical directions, respectively.

The measured optical spectrum and the SHG-based intensity autocorrelation trace of the KLM Yb:SALLO laser are shown in Fig. 4. The optical spectrum of the soliton pulses was centered at 1067.2 nm with a sech^2 -shaped spectral profile (full width at half maximum, FWHM) of 17.5 nm, see Fig. 4(a). The recorded intensity autocorrelation trace was well fitted with a sech^2 -shaped temporal profile yielding a pulse duration of 70 fs, see Fig. 4(b). The corresponding time-bandwidth product (TBP) was 0.322, slightly higher for Fourier-transform limited sech^2 -shaped pulses. The average output power amounted to 271 mW at an absorbed pump power of 1.4 W. The single-pass pump absorption was 29.7% which corresponded to an optical efficiency of 19.4%. The peak on-axis laser intensity in the Yb:SALLO crystal in this situation was calculated to be 258.2 GW/cm². The pulse repetition rate was \sim 80.4 MHz. The pulse duration could not be shortened by reducing the OC transmission, i.e., by applying a 2.5% OC, which indicates the round-trip intracavity GDD of -2400 fs² was insufficient at increased SPM.

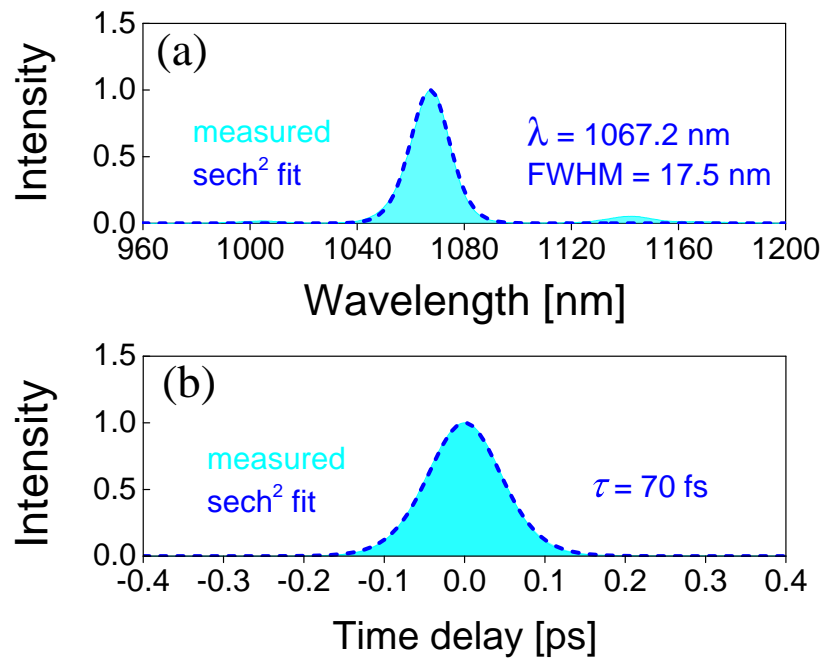


Fig. 4. KLM Yb:SALLO laser with a total negative GDD of -2400 fs² and $T_{OC} = 4\%$. (a) Optical spectrum and (b) SHG-based intensity autocorrelation trace of the output pulses.

Pulse shortening was then realized by removing DM₃ and DM₄ and applying six bounces on DM₁ and DM₂, yielding a total round-trip negative GDD of -3000 fs², as shown in Fig. 2. Using the 4% OC, a single-pulse KLM operation with ultimate stability was achieved after careful cavity alignment. The spectrum of the KLM laser experienced a considerable broadening while displaying a slight deviation from the ideal sech^2 -shaped spectral profile with two sharp satellite peaks at 1100.3 nm and 1120.5 nm, as depicted in Fig. 5(a).

The appearance of these satellite peaks may originate from the unmanageable intracavity GDD at the long-wave spectral wing above 1100 nm and the non-optimized reflection bands of individual cavity mirrors. The laser operated at a central wavelength of 1057.7 nm with an emission bandwidth of 25 nm by assuming a sech^2 -shaped spectral profile. Figure 5(b) shows the

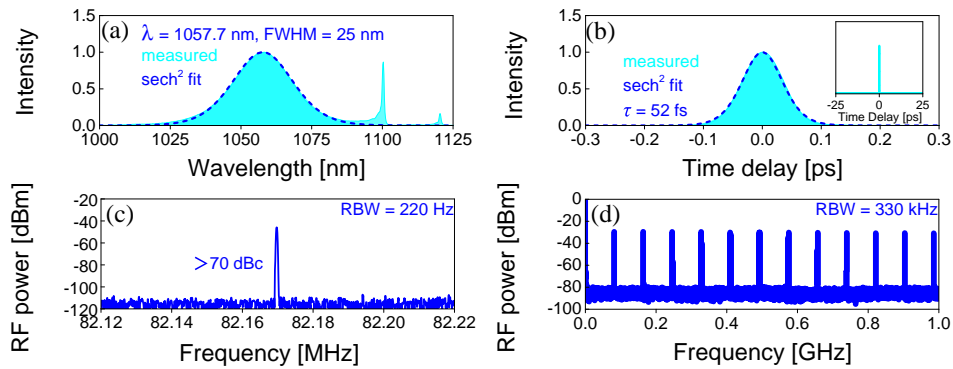


Fig. 5. KLM Yb:SALLO laser with a round-trip GDD of -3000 fs^2 and $T_{OC} = 4\%$. (a) Optical spectrum and (b) SHG-based intensity autocorrelation trace of the shortest pulses. *Inset* in (b): simultaneously measured long-scale (50-ps) autocorrelation trace. RF spectra of the KLM Yb:SALLO laser: (c) fundamental beat note at 82.17 MHz measured with a resolution bandwidth (RBW) of 220 Hz, and (d) harmonics on a 1-GHz span (RBW = 330 kHz).

measured intensity autocorrelation trace of the generated laser pulses. Assuming a sech^2 -shaped temporal profile, the extremely good fit gives a deconvolved pulse duration of 52 fs (FWHM), which leads to a TBP of 0.353, slightly above the Fourier-transform limit for sech^2 -shaped pulses. A long-scale intensity autocorrelation scan of 50 ps is shown in the inset of Fig. 5(b) confirming single-pulse KLM operation without any pedestals or multi-pulses. The maximum average output power amounted to 459 mW at an absorbed pump power of 1.36 W. The cavity length of the KLM Yb:SALLO laser was 1.83 m which corresponded to a pulse repetition rate of 82.17 MHz. The peak on-axis laser intensity in the Yb:SALLO crystal was estimated to be $\sim 576 \text{ GW/cm}^2$. The measured single-pass pump absorption was 26.6% in this condition, which resulted in an optical efficiency of 33.8%. Although the initiation of the ML operation required an external perturbation, the KLM Yb:SALLO laser exhibited ultimate stability once locked. To confirm this, radio-frequency (RF) spectra were recorded, see Figs. 5(c) and (d). The fundamental beat note at 82.17 MHz exhibited a high extinction ratio of $>70 \text{ dBc}$ above the noise level. This, together with the recorded uniform harmonic beat notes on a 1-GHz span is an evidence for stable CW ML operation without any Q-switching or multi-pulsing instabilities.

The pulse duration could be further reduced by increasing the cavity length from 1.83 to 2.27 m which corresponded to a pulse repetition rate of $\sim 66 \text{ MHz}$. After careful alignment, self-starting KLM operation could be achieved with an average output power of 277 mW at an absorbed pump power of 1.07 W. The single-pass pump absorption was 19.4% which resulted in an optical efficiency of 25.9%. The measured optical spectrum and the corresponding intensity autocorrelation trace are shown in Fig. 6(a) and (b), respectively. The soliton pulses had a central wavelength at 1051 nm with a spectral FWHM of 27.6 nm by assuming a sech^2 shaped [see Fig. 6(a)]. Nearly Fourier-limited pulses as short as 44 fs were measured, see Fig. 6(b). The on-axis peak intensity inside the crystal was 511 GW/cm^2 . A long-scale autocorrelation scan of 50 ps was also recorded as can be seen in the inset of Fig. 6(b). Figure 6(c) shows the recorded fundamental beat note at $\sim 66 \text{ MHz}$ with an even higher extinction ratio of $>78 \text{ dBc}$ above the noise level. The harmonic beat notes measured on a 1-GHz span remained uniform as can be seen in Fig. 6(d).

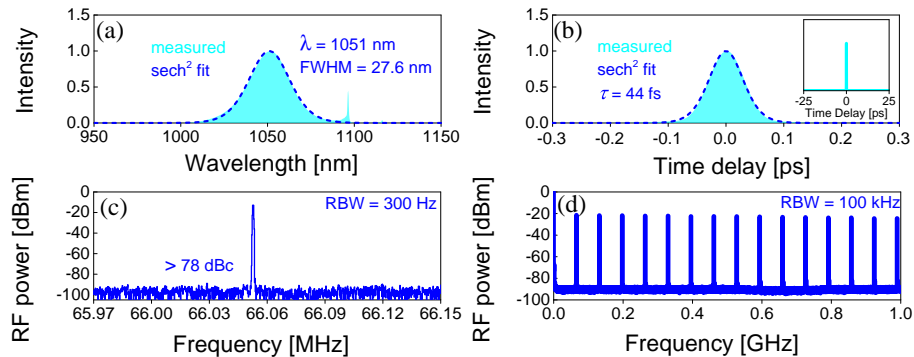


Fig. 6. KLM Yb:SALLO laser with a round-trip GDD of -3000 fs^2 and $T_{OC} = 4\%$. (a) Optical spectrum and (b) SHG-based intensity autocorrelation trace of the shortest pulses. *Inset* in (b): simultaneously measured long-scale (50-ps) autocorrelation trace. RF spectra of the KLM Yb:SALLO laser: (c) fundamental beat note at $\sim 66 \text{ MHz}$ measured with a resolution bandwidth (RBW) of 300 Hz, and (d) harmonics on a 1-GHz span (RBW = 100 kHz).

4. Conclusion

In conclusion, we demonstrate the first KLM operation of the Yb:SALLO laser in the sub-100 fs time domain. Using a 4% OC, nearly Fourier-transform limited pulses as short as 44 fs were generated at 1051 nm from the Yb:SALLO laser pumped by a high-brightness fiber laser via soft-aperture Kerr-lens mode-locking. A higher average output power of 459 mW was obtained at the expense the pulse duration (52 fs) for a pulse repetition rate of $\sim 82.17 \text{ MHz}$. This corresponded to a relatively high optical efficiency of 33.8% in the ML regime. Our results indicate the possibilities of further power scaling and pulse shortening in ML Yb:SALLO lasers through optimized pump absorption, i.e., zero-phonon line pumping, fine control of the intracavity GDD over the entire spectral bandwidth, and optimized reflectivity bands of the cavity mirrors. This new material is expected to develop into a viable alternative to the CALGO/CALYO hosts studied in ML Yb lasers for more than 15 years.

Funding. National Natural Science Foundation of China (61975208, 51761135115, 61850410533, 62075090, 52032009, 52072351); Sino-German Scientist Cooperation and Exchanges Mobility Program (M-0040); Foundation of President of China Academy of Engineering Physics (YZJLX2018005); Foundation of Key Laboratory of Optoelectronic Materials Chemistry and Physics, Chinese Academy of Sciences (2008DP173016); Foundation of State Key Laboratory of Crystal Materials, Shandong University (KF2001).

Disclosures. The authors declare no conflicts of interest.

Data availability. Data underlying the results presented in this paper are not publicly available at this time but may be obtained from the authors upon reasonable request.

References

1. A. Pajczkowska and A. Gloubokov, "Synthesis, growth and characterization of tetragonal ABCO_4 crystals," *Prog. Cryst. Growth Charact. Mater.* **36**(1-2), 123–162 (1998).
2. P. Petit, J. Petit, P. Goldner, and B. Viana, "Inhomogeneous broadening of optical transitions in Yb:CaYAlO₄," *Opt. Mater.* **30**(7), 1093–1097 (2008).
3. J. Petit, P. Goldner, and B. Viana, "Laser emission with low quantum defect in Yb:CaGdAlO₄," *Opt. Lett.* **30**(11), 1345–1347 (2005).
4. D. Li, X. Xu, H. Zhu, X. Chen, W. De Tan, J. Zhang, D. Tang, J. Ma, F. Wu, and C. Xia, "Characterization of laser crystal Yb:CaYAlO₄," *J. Opt. Soc. Am. B* **28**(7), 1650–1654 (2011).
5. P. Loiko, F. Druon, P. Georges, B. Viana, and K. Yumashev, "Thermo-optic characterization of Yb:CaGdAlO₄ laser crystal," *Opt. Mater. Express* **4**(11), 2241–2249 (2014).
6. F. Druon, M. Olivier, A. Jaffrès, P. Loiseau, N. Aubry, J. DidierJean, F. Balembois, B. Viana, and P. Georges, "Magic mode switching in Yb:CaGdAlO₄ laser under high pump power," *Opt. Lett.* **38**(20), 4138–4141 (2013).

7. P. Loiko, J. M. Serres, X. Mateos, X. Xu, J. Xu, V. Jambunathan, P. Navratil, A. Lucianetti, T. Mocek, and X. Zhang, "Microchip Yb:CaLnAlO₄ lasers with up to 91% slope efficiency," *Opt. Lett.* **42**(13), 2431–2434 (2017).
8. P. Sévillano, P. Georges, F. Druon, D. Descamps, and E. Cormier, "32-fs Kerr-lens mode-locked Yb:CaGdAlO₄ oscillator optically pumped by a bright fiber laser," *Opt. Lett.* **39**(20), 6001–6004 (2014).
9. A. Diebold, F. Emaury, C. Schriber, M. Golling, C. J. Saraceno, T. Stüdmeyer, and U. Keller, "SESAM mode-locked Yb:CaGdAlO₄ thin disk laser with 62 fs pulse generation," *Opt. Lett.* **38**(19), 3842–3845 (2013).
10. W. Tian, R. Xu, L. Zheng, X. Tian, D. Zhang, X. Xu, J. Zhu, J. Xu, and Z. Wei, "10-W-scale Kerr-lens mode-locked Yb:CALYO laser with sub-100-fs pulses," *Opt. Lett.* **46**(6), 1297–1300 (2021).
11. J. Yang, Z. Wang, J. Song, R. Lv, X. Wang, J. Zhu, and Z. Wei, "Diode-pumped 10 W femtosecond Yb:CALGO laser with high beam quality," *High Power Laser Sci. Eng.* **9**, e33 (2021).
12. W. Tian, C. Yu, J. Zhu, D. Zhang, Z. Wei, X. Xu, and J. Xu, "Diode-pumped high-power sub-100 fs Kerr-lens mode-locked Yb:CaYAlO₄ laser with 1.85 MW peak power," *Opt. Express* **27**(15), 21448–21454 (2019).
13. W. Tian, G. Wang, D. Zhang, J. Zhu, Z. Wang, X. Xu, J. Xu, and Z. Wei, "Sub-40-fs high-power Yb:CALYO laser pumped by single-mode fiber laser," *High Power Laser Sci. Eng.* **7**, e64 (2019).
14. S. Manjooran and A. Major, "Diode-pumped 45 fs Yb:CALGO laser oscillator with 1.7 MW of peak power," *Opt. Lett.* **43**(10), 2324–2327 (2018).
15. Y. Wang, X. Su, Y. Xie, F. Gao, S. Kumar, Q. Wang, C. Liu, B. Zhang, B. Zhang, and J. He, "17.8 fs broadband Kerr-lens mode-locked Yb:CALGO oscillator," *Opt. Lett.* **46**(8), 1892–1895 (2021).
16. J. Ma, F. Yang, W. Gao, X. Xiaodong, X. Jun, D. Shen, and D. Tang, "Sub-five-optical-cycle pulse generation from a Kerr-lens mode-locked Yb:CaYAlO₄ laser," *Opt. Lett.* **46**(10), 2328–2331 (2021).
17. Z. B. Pan, X. J. Dai, Y. H. Lei, H. Q. Cai, J. M. Serres, M. Aguilo, F. Diaz, J. Ma, D. Y. Tang, E. Vilejshikova, U. Griebner, V. Petrov, P. Loiko, and X. Mateos, "Crystal growth and properties of the disordered crystal Yb:SrLaAlO₄: a promising candidate for high-power ultrashort pulse lasers," *Crystengcomm.* **20**(24), 3388–3395 (2018).
18. W. Ryba-Romanowski, S. Gołab, I. Sokolska, W. Pisarski, G. Dominiak-Dzik, A. Pajęczkowska, and M. Berkowski, "Anisotropy of optical properties of SrLaAlO₄ and SrLaAlO₄: Nd," *J. Alloy. Compd.* **217**(2), 263–267 (1995).
19. D. Adhikari, M. M. Junda, P. Uprety, K. Ghimire, I. Subedi, and N. J. Podraza, "Near infrared to ultraviolet anisotropic optical properties of single crystal SrLaAlO₄ from spectroscopic ellipsometry," *Physica Status Solidi A* **253**(10), 2066–2072 (2016).